J Mater Sci: Mater Med (2011) 22:1843–1853
DOI 10.1007/s10856-011-4367-7

Fabrication and characterization of interconnected porous biodegradable poly(ε-caprolactone) load bearing scaffolds

Rula M. Allaf · Iris V. Rivero

Received: 10 November 2010 / Accepted: 30 May 2011 / Published online: 14 June 2011

Abstract In this study, poly(ε-caprolactone) (PCL)/poly(ethylene oxide) (PEO) (50:50 wt%) immiscible blend was used as a model system to investigate the feasibility of a novel solventless fabrication approach that combines cryomilling, compression molding and porogen leaching techniques to prepare interconnected porous scaffolds for tissue engineering. PCL was cryomilled with PEO to form blend powders. Compression molding was used to consolidate and anneal the cryomilled powders. Selective dissolution of the PEO with water resulted in interconnected porous scaffolds. Sodium chloride salt (NaCl) was subsequently added to cryomilled powder to increase the porosity of scaffolds. The prepared scaffolds had homogeneous pore structures, a porosity of ~50% which was increased by mixing salt with the blend (~70% for 60% wt% NaCl), and a compressive modulus and strength ($\varepsilon = 10\%$) of 60 and 2.8 MPa, respectively. The results of the study confirm that this novel approach offers a viable alternative to fabricate scaffolds.

1 Introduction

Tissue engineering/regenerative medicine has been a topic of extensive research over the last few decades. It is an emerging multidisciplinary field that applies principles and methods of life sciences and engineering towards the understanding of structure–function relationships in normal and pathological mammalian tissues; in addition to the development of biological substitutes, typically composed of biological and synthetic components, for restoring, maintaining, or enhancing tissue and organ function [1, 2]. In tissue engineering, cell populations that are usually expanded by culturing and bioactive factors (e.g. growth factors, cytokines, and DNA fragments) are seeded onto a biodegradable scaffold or matrix that supports and guides the proliferation of new cells in three dimensions (3D). Material selection and fabrication techniques provide two important cornerstones for tissue engineering practices. A biocompatible, biodegradable, bioresorbable, and interconnected porous scaffold or matrix is designed as a carrier for cells and growth factors to be implanted to repair damaged tissue; as a template to define new tissue growth in 3D; and as a temporary substitute providing normal tissue functional properties and degrading at the appropriate rate to allow tissue regeneration [3, 4]. Scaffolds have been fabricated from natural biomaterials, synthetic biocompatible materials, blends or composites using a number of processing techniques such as solvent casting combined with particulate leaching [5], freeze drying [6], super-critical fluid technology [7], phase separation [8], fiber bonding [9], melt molding combined with particulate leaching [10, 11], solid freeform fabrication [12, 13], and combinations of these techniques, especially with particulate leaching to increase porosity and pore interconnectivity.

Recently, a new porogen methodology for the preparation of porous scaffolds has emerged from the melt blending, typically in an extruder or mixer, of two immiscible polymers in the composition range, close to the phase inversion point, that is required to create co-continuous blend morphologies [14–19]. This co-continuous morphology, a biphasic structure in which each phase is fully continuous (interconnected), generally occurs in the 40:60–60:40 (vol.%) composition range [14]. Subsequently, leaching one of the polymer phases using a selective

R. M. Allaf · I. V. Rivero (✉)
Department of Industrial Engineering, Texas Tech University, Lubbock, TX 79409-3061, USA
e-mail: iris.rivero@ttu.edu

solvent, this is feasible due to the full continuity of the two phases, results in a porous structure with fully interconnected pores [14, 15]. This polymer porogen leaching method results in a cylindrical pore interconnection structure that is completely different from that observed with the other scaffold fabrication techniques where the larger pores are generally interconnected through smaller gates [14]. This pore network structure results in scaffolds that are particularly suitable for load bearing applications such as bone or cartilage regeneration [14]. The size-scale of the blend phase domains, hence the pore size, can generally be greatly increased by annealing above the melting temperature (semi-crystalline polymer) or glass transition temperature (amorphous polymer) of the two components [14–16, 18]. The pore size can be controlled from fraction of microns to hundreds of microns. The upper limit of pore size is in the range required for scaffolds for tissue engineering (5–400 μm) [18]. However, one drawback of the technique is that it yields maximum porosity of 50–60%. Reignier and Huneault [14] combined polymer leaching with particulate leaching in order to overcome this limitation achieving porosities between 75 and 88% in a bimodal pore size distribution. Poly(ethylene oxide) (PEO) [14, 15], polystyrene (PS) [16, 17, 19], poly(ε-caprolactone) (PCL) [18], and poly-L-lactic acid (PLLA) [18] polymer porogens have been used to make porous PCL, PLLA, and polyglycolic acid (PGA) structures from model blends of PCL/PEO, PLLA/PS, PLLA/PCL, and PGA/PLLA, respectively.

Melt blending becomes inefficient in achieving homogeneous blending when the polymer melts are highly viscous [20], a polymer does not melt at all [21], or when adding a filler to the blend with a high loading [20]. Furthermore, other disadvantages of melt blending include degradation of polymers at high temperatures, undesirable chemical reactions, and unstable morphologies [22]. Solid state blending provides an attractive alternative to melt blending to produce blends and composites. Solid state processing methods utilize high amounts of shear and/or compressive forces below the melt and/or glass transition temperatures of the polymer and the filler to produce intimate mixtures or alloys. A number of solid-state processing methods have been investigated for the production of polymer blends and composites, including mechanical alloying [22, 23], pan-milling mixing [24], and solid-state shear pulverization [25, 26].

Mechanical alloying is a high energy ball milling process in which powders placed in a vial with balls are repeatedly fractured, deformed, and welded due to high energy impacts between balls, powders, and vial walls; thus, enabling alloy powders to be formed from mixtures of elemental powders [27]. To embrittle the polymer and overcome its viscoelasticity, milling can be performed at cryogenic temperatures usually in liquid nitrogen (approximately −196°C); this adapted technology is known as cryogenic mechanical alloying or cryomilling [20]. Cryomilling has proven to improve the blending intimacy, enhance compatibility between the different blend components, and increase the degree of dispersion in polymer composites [20, 28], in addition to reducing and narrowing overall particle size distributions [29] and promoting a physical reduction in the scale of mixing [30].

The present study is designed to explore the efficacy of homogeneous blending of PCL and PEO by cryomilling and to devise a viable and economical route through which highly interconnected 3D porous scaffolds can be molded. In this study, homogeneity of blending is established by the uniformity of the interconnected morphology, and hence the resulting mechanical properties. The PCL/PEO system is ideally suited for the present study, which seeks to produce scaffolds for tissue engineering using biodegradable polymers through the integration of cryomilling, compression molding, and porogen leaching techniques. PCL is a biodegradable, soft- and hard-tissue biocompatible material with easy processability [31]. It is a highly crystallizable aliphatic polyester, where crystals reinforce the PCL enhancing its mechanical properties [32]. PCL can be degraded by hydrolysis of the ester linkages in its chains under physiological conditions; it has shown remarkable long in vivo degradation [33], which is very well-suited with cartilage tissue limited healing ability. Furthermore, cryomilling is intended to blend PCL with other polymers to manipulate its properties and degradability.

PEO is a biodegradable water soluble polymer known to be immiscible with PCL and to form co-continuous PCL/PEO structures by melt blending in the 30:70–60:40 (vol%) composition range [14, 15]. Therefore, PEO is a suitable polymer porogen for the PCL scaffold. PEO provides two advantages: first, as a water soluble polymer, potentially toxic organic solvents are not necessary to dissolve PEO. Second, being biocompatible and biodegradable, small amounts of residual PEO can be endured in the final porous scaffold.

Results from this study aim to establish a scaffold structure suitable for load bearing application. In addition, this approach will lead to a scaffold fabrication procedure which can eventually be used to produce homogeneous fully interconnected porous composite scaffolds with well-dispersed fillers and tunable properties, without the use of the potentially harmful organic solvents.

2 Materials and methods

2.1 Materials

Poly(ε-caprolactone) powder (Perstorp UK Limited, only 2% above 600 μm) with a number average molecular

weight (M_n) of 47500, a density of 1.1 g/cm^3 (at 60°C), a melt flow index of 5.20–11.3 g/10 min (1″ PVC die, 160°C, 2.16 kg), and a melting temperature range of 58–60°C was used in this study. Poly(ethylene oxide) fine powder (Sigma-Aldrich, Mesh −20, 96–100%) with a viscosity average molecular weight (M_v) of 100000, a density of 1.13 g/cm^3 (at 25°C), a viscosity of 12–50 cP (at 25°C, C = 5%, H_2O), a glass transition temperature of −67°C, and a melting temperature of 65°C was utilized as a biodegradable polymer porogen. Non-medical polymer grades were used in this study since no in vivo studies were planned at this stage. Table salt (NaCl) was also used as a particulate porogen in the study.

2.2 Powder milling

To establish the effectiveness of cryomilling in producing co-continuous blends, a series of 50:50 wt% PCL/PEO blends have been milled. The PCL/PEO composition ratio was chosen at 50:50 to ensure a co-continuous morphology of the polymer components [14]. Blending was performed using a SPEX 6770 SamplePrep Freezer mill (SPEX CertiPrep Group, Inc., USA), which cools samples to cryogenic temperatures using liquid nitrogen, and pulverizes them by magnetically shuttling a steel impactor back and forth in a polycarbonate vial against two stationary steel end plugs. PCL and PEO powders were first manually mixed in a 50:50 wt% ratio to obtain 1.5 g samples. Subsequently, the 1.5 g powder samples were cryogenically milled for 30 min of actual milling, using the following parameters: 15 min of pre-cooling, 2 min of cooling between every 3 min of continuous milling, and a frequency of 10 cycles per second (cps). Parameters were selected based on SPEX recommendations and Terife and Narh study [34] which also used 30 min of cryomilling to produce PEO nanocomposites. Furthermore, 30 min were also adequate to disperse Mg–Al hydrotalcite in a PCL matrix enhancing its mechanical properties despite a small reduction in its molecular weight [35]. Therefore, 30 min of cryomilling was chosen to examine the production of homogeneous blends without much degradation.

NaCl was later manually mixed with a cryomilled PCL/PEO sample in a 60:40 wt% ratio to investigate the ability to increase scaffold porosity by adding salt to the blend. Furthermore, the NaCl concentration was selected at 60 wt%, which is lower than the value reported for complete salt extraction in PCL/NaCl mixtures (~74 wt%) [14], to explore enhanced scaffold pore interconnectivity at a low volume fraction of NaCl porogen particles using this fabrication approach.

Scanning electron microscopy (SEM) micrographs of preground PCL, PEO, and NaCl particles and PCL/PEO cryomilled blends are shown in Figs. 1 and 2, respectively. Resultant cryomilled PCL/PEO flake size ranged from ~32 μm to ~944 μm, with an average size of ~214 μm.

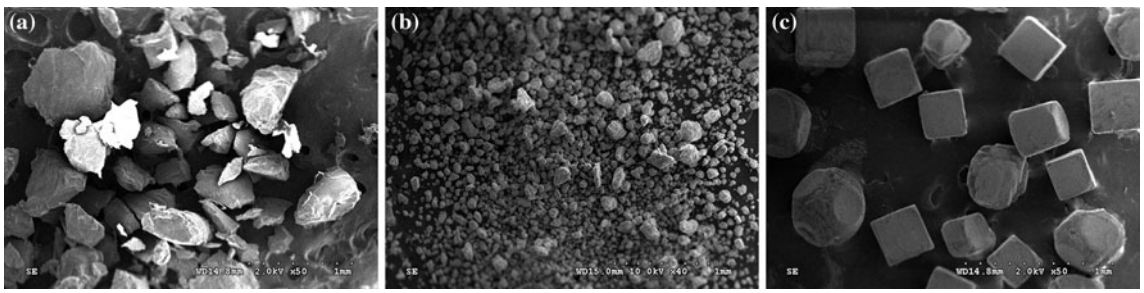

Fig. 1 SEM micrographs of **a** preground PCL, **b** preground PEO, and **c** NaCl particles

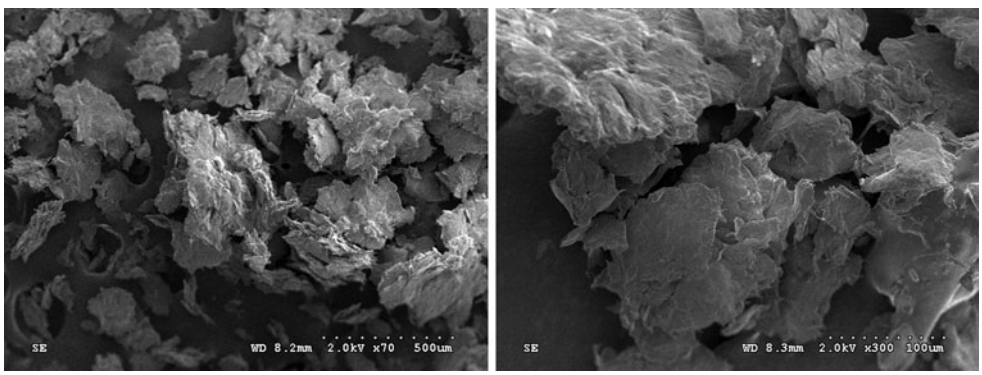

Fig. 2 SEM micrographs of PCL/PEO powders cryomilled for 30 min. Two magnifications are shown

2.3 Compression molding

Cryomilled powders were consolidated in a Carver bench top laboratory press (Carver, Inc., Wabash, IN) at two different temperatures: 60 and 100°C to investigate the effect of compression temperature on the products' properties. These temperatures were chosen at and above the polymers' melting temperatures to promote consolidation of powders, motion of polymer chains, segregation of phases, and then coarsening. Powder samples were loaded in a mold and compression molded into 9 mm diameter cylinders with 13 mm height. The mass loadings of the different compositions were calculated to fill the mold cavity so that a constant volume of 827 mm^3 was achieved for each sample, assuming homogeneous powder composition and using the following polymer densities: $\rho_{PCL} = 1.14$ g/mm^3 and $\rho_{PEO} = 1.13$ g/mm^3.

The compression molding cycle is described as follows: during the initial 15–20 min period of the cycle, a 226.8 kgf was applied and stabilized to compact the powders and remove the entrapped air. Heat was then applied while still maintaining the pressure and the powders were left at the molding temperature for 30 min, after which the heat was turned off and the powders were allowed to cool down for 1 h before the pressure was released. Subsequently, the mold was cooled to room temperature in a water bath and samples were then removed from the mold. Four samples were compressed in each molding cycle.

2.4 Scaffold leaching and drying

After cooling, the samples were immersed in water in 15 ml vials in a water bath, at room temperature, in order to dissolve the water soluble porogen(s). The water was changed every day until the wet sample achieved constant weight. After porogen extraction, the samples were removed from water, blotted dry, and placed in a vacuum oven at 45°C for 4 days until no change in dry sample weight was detected. The mass and dimensions of each sample were measured after the molding, leaching, and drying processes. Five measurements of the samples' diameters and heights were taken with an electronic caliper and were then averaged for the volume calculations. Figure 3 summarizes the scaffold fabrication approach.

2.5 Scaffold characterization

2.5.1 Porosity, PEO continuity, and morphology

The porosity was measured using a gravimetric method. The method is based on the assumption that only porogens are completely extracted out due to the co-continuous structure of the PCL/PEO blends confirmed via scanning electron microscopy (SEM) imaging. Thus porosity was calculated using the following equation [6, 14]:

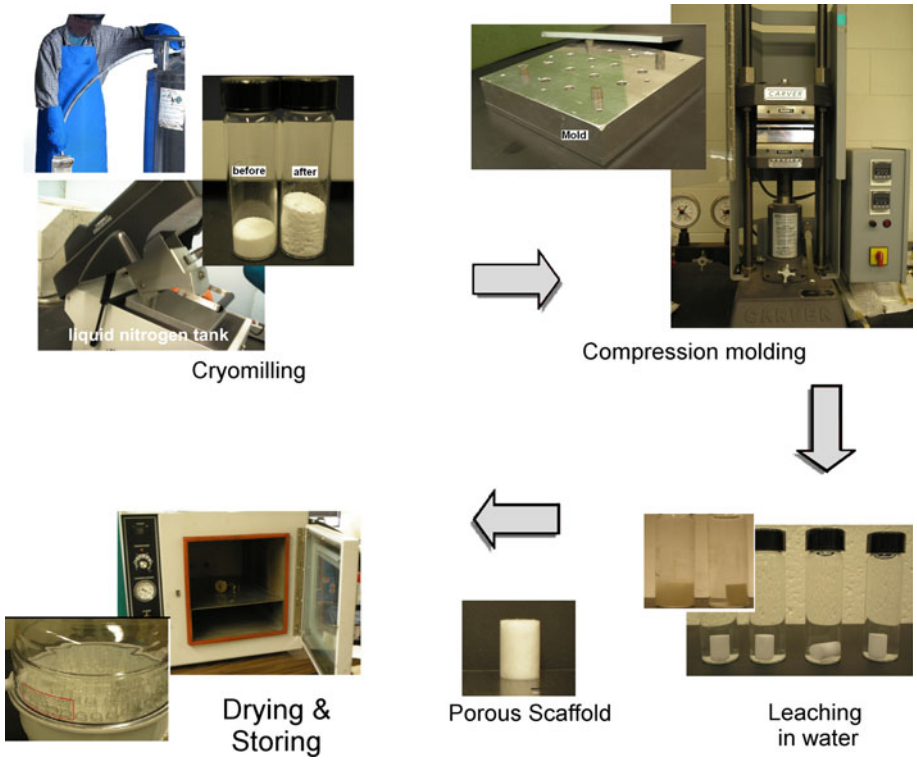

Fig. 3 Photographs showing complete scaffold fabrication approach

$$\text{Porosity}(\%) = \left(1 - \frac{V_{\text{PCL}}}{V_{\text{scaffold}}}\right) \times 100\% = \left(1 - \frac{\rho_{\text{scaffold}}}{\rho_{\text{PCL}}}\right) \times 100\% \quad (1)$$

where ρ_{scaffold} (g/mm^3) is the apparent density of the scaffold measured by dividing the weight by the volume of the scaffold and ρ_{PCL} (g/mm^3) is the density of the non porous PCL material from which the scaffold was made ($\rho_{\text{PCL}} = 1.14$ g/mm^3).

Weight-loss measurements were carried out to evaluate the extent of continuity of PEO using the following equation [14, 18]:

$$\%\,\text{Continuity of PEO} = \frac{\text{weight PEO}_{\text{initial}} - \text{weight PEO}_{\text{final}}}{\text{weight PEO}_{\text{initial}}} \times 100\% \quad (2)$$

where weight $\text{PEO}_{\text{initial}}$ corresponds to the weight of PEO in the sample before the extraction step, and weight $\text{PEO}_{\text{final}}$ corresponds to weight of PEO remaining in the sample after extraction, both calculated from the weight fraction of PEO in the blend assuming homogeneous blends.

The morphologies of scaffolds were examined with a Hitachi S-4300 SE/N high-resolution field emission scanning electron microscope (FESEM, Hitachi, Japan) operated at accelerating voltages of 2, 10 and 15 kV (aperture 2) in secondary and environmental modes. Samples were fractured in liquid nitrogen to observe the cross sectional morphologies. Specimens were mounted on the SEM holder using an aluminum stub with double-sided carbon tape. Image analysis was carried out using SIMAGIS software (Smart Imaging Technologies, USA) in order to obtain quantitative information on scaffold morphology. SEM micrographs were analyzed to estimate average pore diameter. On average, about 30 pores were measured for each image, taking two diameters per pore to account for elliptical pores.

2.5.2 *Compressive mechanical testing*

Uniaxial unconfined compression mechanical testing was performed using a TestResources universal testing machine (TestResources Inc., Shakopee, MN, USA) at room temperature with a 453.6 kgf load cell. Cylindrical samples were compressed at a cross-head speed of 1 mm/min for 10 mm from sample's initial height. The change in height and the force applied to the sample were measured as well as the sample's non-deformed length and cross sectional area. Elastic compressive modulus and compression strength of the sample were determined using calculated stress–strain diagrams. The modulus (E) was determined by linear regression analysis as the slope of the first linear region of the stress–strain curve and the compressive strength ($\sigma_{\varepsilon=0.1}$) was measured at ~10% strain in the plateau region [19] after toe region correction for the zero-strain point (Fig. 4).

2.5.3 *Differential scanning calorimetry*

The thermal properties of scaffolds were evaluated by differential scanning calorimetry (DSC). Samples (6–10 mg) were cut from scaffolds, placed in 40 µl aluminum pans, and analyzed with a Mettler Toledo 823e differential scanning calorimeter (Mettler-Toledo Inc., Columbus, OH, USA) equipped with an intracooler under a nitrogen purge at a heating rate of 10°C/min. The instrument was calibrated with indium for melting point and heat of fusion. Samples were heated from −20 to 100°C, held at 100°C for 3 min, then subsequently cooled to −20°C at −10°C/min and after 3 min a second heating scan was applied. The resulting DSC curves were analyzed to determine transition temperatures and degree of crystallinity. The degree of crystallinity (Xc) was determined by the fusion enthalpy method using the following equation [18]:

$$\text{Xc}(\%) = \frac{\Delta H_m}{\Delta H_m^\circ} \times 100\% \quad (3)$$

where ΔH_m and ΔH_m° designate the measured melting enthalpy and the melting enthalpy of 100% crystalline PCL, using $\Delta H_m^\circ = 139.5$ J/g [11], respectively.

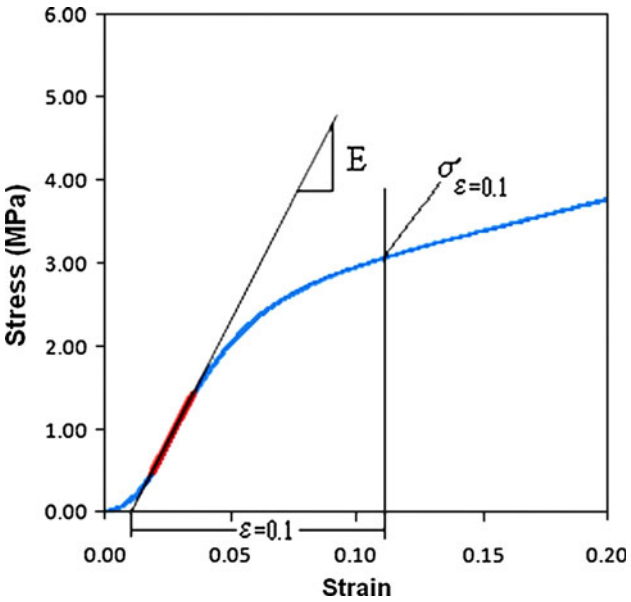

Fig. 4 Methodology for determining the elastic modulus (E) and the compressive strength ($\sigma_{\varepsilon=0.1}$) of scaffolds from the stress–strain diagram

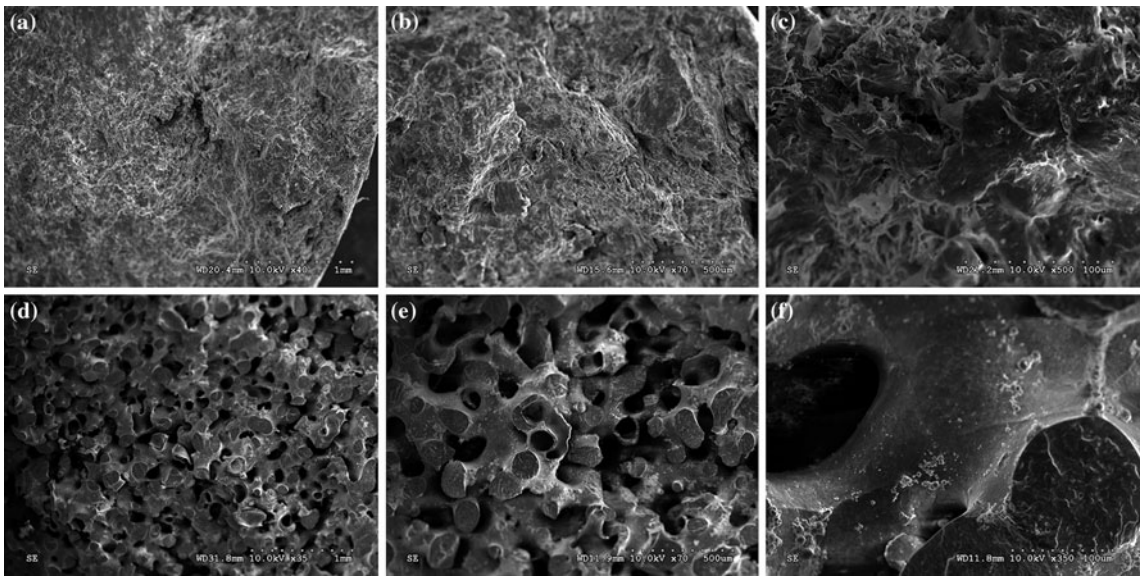

Fig. 5 SEM micrographs of PCL/PEO powders cryomilled for 30 min and compression molded at **a**, **b**, **c** 60°C and **d**, **e**, **f** 100°C. Three magnifications are shown. The low magnifications (**a**, **b**, **d**, **e**) reveal the pore morphology and the higher magnifications (**c**, **f**) show the texture in the pore walls

3 Results

3.1 Porosity, PEO continuity, and morphology

3.1.1 Effect of compression temperature

The results of porosity calculations showed that porosities achieved at 60 and 100°C were 45.9% ± 1.3% and 49.8% ± 1.4%, respectively. Furthermore, continuity evaluations showed that PEO continuity achieved at 60 and 100°C were 97.0% ± 0.6% and 97.6% ± 0.5%, respectively; equivalently stated as 48.6% ± 0.3% reduction in scaffold weight. However, morphological observations (Fig. 5) showed that the pore morphology obtained varied significantly between the two different compression temperatures. Scaffolds molded at 60°C exhibited small pores along with a rough flaky lamellar texture (Fig. 5a–c); whereas those molded at 100°C demonstrated an apparently homogeneous, interconnected pore structure with an average pore size of ~140 μm (Fig. 5d–f). In other words, the scaffolds structure is characterized by the coexistence of an interconnected network of cylindrical pores and an interconnected network of PCL cylinders. This co-continuous morphology is confirmed by the porosity and continuity results which showed that the PEO phase was almost completely extracted out while still maintaining the integrity of the porous PCL phase (PCL scaffold is self supporting). It is also obvious that the PCL walls exhibited a smooth texture.

3.1.2 Effect of salt addition

Addition of salt to the PCL/PEO cryomilled powder sample, which was subsequently molded at 60°C, resulted in an increase of porosity from 45.9 to 69.3%, with a PEO continuity evaluated at 91.8%. Morphological observations (Fig. 6) showed that the pore morphology obtained primarily resembled the NaCl particles size and shape, with an average pore size of ~320 μm and all NaCl dissolved. Pores of smaller sizes were also observed, which may have been created by contact between salt particles before leaching. Higher magnification images (Fig. 6c) revealed that the pore wall surface had the same rough flaky lamellar texture as the PCL scaffold (Fig. 5c) fabricated from the PCL/PEO blend molded at the same temperature (60°C).

For comparison purposes, porosity measurements were also investigated on PCL/NaCl binary blends compression molded using the same molding process. In that case, the porosity achieved for a scaffold molded at 60°C was 13.6% (expected porosity from complete NaCl extraction was 50%), which is clearly explained by the SEM image (Fig. 7) that shows salt particles still entrapped in the scaffold after leaching.

3.2 Compressive mechanical properties

The results of the compression tests were interpreted in terms of stress–strain curves. Typical curves are shown in Fig. 8 for the various fabricated scaffolds. These curves

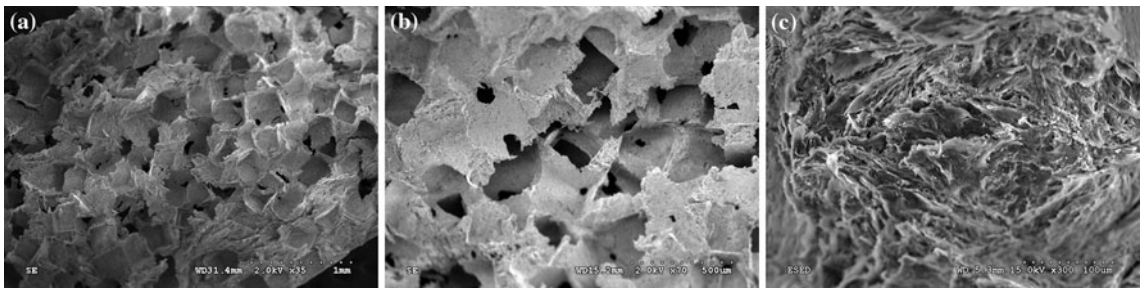

Fig. 6 SEM micrographs of PCL/PEO/NaCl powders cryomilled for 30 min and compression molded at 60°C. Three magnifications are shown. The low magnifications (**a**, **b**) reveal the pore morphology and the higher magnification (**c**) shows the texture in the pore walls

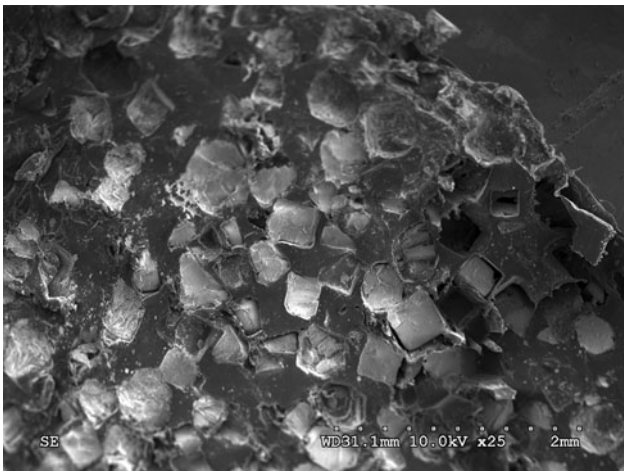

Fig. 7 SEM micrographs of PCL/NaCl (35:65 wt%) powders manually mixed and compression molded at 60°C

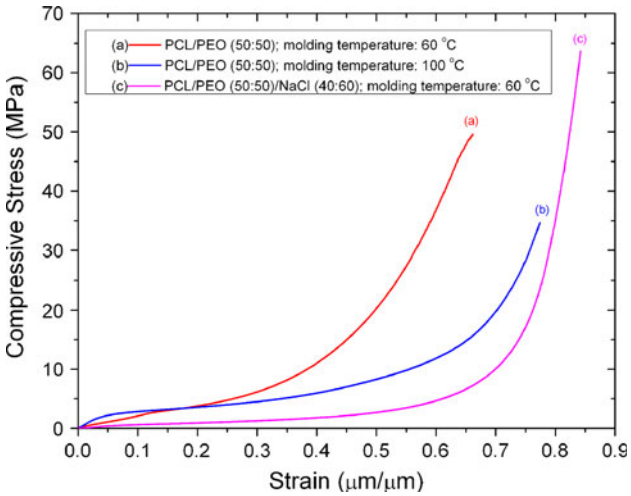

Fig. 8 Compression stress strain curves for PCL scaffolds made from (*a*) PCL/PEO (50:50) compression molded at 60°C, (*b*) PCL/PEO (50:50) powders compression molded at 100°C, (*c*) PCL/PEO (50:50) powders cryomilled for 30 min, mixed with NaCl (40:60) and compression molded at 60°C

show typical behavior of polymeric foams under compression. Values of elastic modulus and compressive strength at 10% strain derived from the stress–strain curves are listed in Table 1.

3.3 Thermal properties

The DSC thermal analysis was conducted between −20°C and 100°C in three scans, 1st heating, cooling, and 2nd heating, to enable the collection of information about the physical structure developed during processing due to the thermal and mechanical histories in addition to material properties. The DSC thermograms for the heating scans are shown in Fig. 9. Table 2 summarizes the main information derived from the DSC heating and cooling scans. From the first heating scans, the onset and peak melting temperatures (Tm_{onset} and Tm_{peak}) of PCL after molding at 60°C were 51.6 and 57.3°C, respectively; whereas after molding at 100°C, they were 57.9 and 65.8°C, respectively. Furthermore, crystallinities (Xc) achieved at 60 and 100°C were 63.3 and 83.2%, respectively. PCL from scaffolds fabricated with salt addition showed an onset and peak melting temperatures of 57.6 and 67.6°C, respectively, in addition to a crystallinity of 73.1%. Second heating and cooling scans showed more comparable values associated with PCL material properties. Those values were also similar to those obtained for PCL after molding at 60°C (1st scan).

4 Discussion

In the current fabrication protocol, scaffolds were prepared by cryomilling mixtures of PCL/PEO (50:50 wt%) for 30 min followed by compression molding at two different temperatures (60 and 100°C), and then porogen leaching to investigate the feasibility of the suggested approach at producing interconnected porous scaffolds. The temperature was set at and over the polymers melting temperature to promote consolidation of powders and segregation of phases. Pressure was applied before and during heating to compact the powders and remove entrapped air porosity.

Table 1 Compressive property of various PCL porous scaffolds

Composition and molding temperature	Compressive modulus (MPa)	Compressive strength ($\varepsilon = 0.1$) (MPa)
PCL/PEO (50:50); 60°C	19[a]	2.1[a]
PCL/PEO (50:50); 100°C	60 ± 0.3[b]	2.8 ± 0.01[b]
PCL/PEO (50:50)/NaCl (40:60); 60°C	8 ± 0.2[b]	0.6 ± 0.01[b]

[a] Single replicate

[b] Standard error of mean

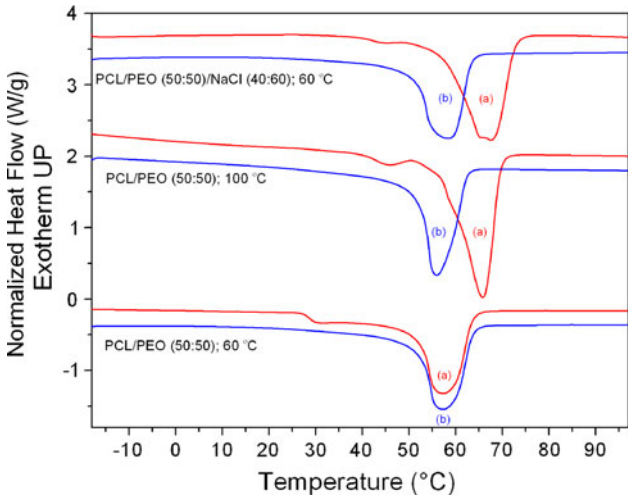

Fig. 9 DSC (*a*) first heating and (*b*) second heating scans for PCL scaffold samples recorded at 10°C/min

Table 2 DSC melting and crystallization data for PCL scaffold samples

	Composition and molding temperature		
	PCL/PEO (50:50); 60°C	PCL/PEO (50:50); 100°C	PCL/PEO (50:50)/ NaCl (40:60); 60°C
1st heating scan			
Tm_{peak} (°C)	57.3	65.8	67.6
Tm_{onset} (°C)	51.6	57.9	57.8
ΔHm (J/g)	−88.32	−116.07	−101.93
Xc (%)	63.3	83.2	73.1
2nd heating scan			
Tm_{peak} (°C)	57.3	55.9	58.4
Tm_{onset} (°C)	51.9	52.1	51.2
ΔHm (J/g)	−85.8	−83.05	−83.68
Xc (%)	61.5	59.5	60.0
Cooling scan			
Tc_{peak} (°C)	30.8	29.4	29.5
Tc_{onset} (°C)	34.1	33.0	33.3
ΔHc (J/g)	79.32	78.20	75.22

Scaffolds were fabricated with different structures and mechanical properties. The morphology of scaffolds fabricated at 60°C exhibited a rough flaky lamellar texture and random small pores. Scaffolds fabricated at 100°C clearly showed a typical co-continuous porous structure with cylindrical interconnected pores. In polymer leaching techniques, pore size obtained is dictated by the scale of segregation in the co-continuous polymer blend [14]. This will depend on the size and scale of mixing of the cryo-milled powders, and the degree of coarsening that occurs during molding, which in turn are governed by cryomilling time and molding temperature and pressure, respectively. Molding at the melting temperature of PCL (60°C) was not enough to induce phase segregation and coarsening. As the blend was pressed and annealed at a higher temperature (100°C), the inherent immiscibility of PCL and PEO was manifested, phase coarsening proceeded, and thus pore size increased. These results further demonstrate the high degree of mixing in these blends obtained by cryogenic milling. The presence of PEO small droplets in the PCL matrix (Fig. 5f) could clarify why the PEO interconnectivity is lower than 100%.

Well interconnected structures such as those shown in Fig. 5d-f are indispensable in tissue engineering to allow cell migration and proliferation, and extracellular matrix production [14], as well as to supply nutrients for cell growth and transport of metabolic waste products [14, 36]. Interconnection between pores is also important for complete porogen extraction during leaching [14]. Pore size and pore throats are also important for cell survival, since they govern permeability and diffusivity throughout the scaffold, in addition to mechanical integrity. Increased pore opening size is desirable to improve cell seeding throughout the whole scaffold and not only on its surface [14], since cells or cell aggregates larger than the pore openings cannot penetrate deeply into the scaffold. The average pore size obtained in this study is within the optimum pore size values (5–400 μm) reported in the tissue engineering literature [18]. Additionally, pore shape and wall roughness are important factors for better cell spreading [36].

Addition of salt to the PCL/PEO cryomilled sample resulted in an increase of porosity in a rough macro-porous topography. This rough texture could play an important role in regulating cell-scaffold interactions. The properties of scaffold surface micro-topography are thought to influence the localization and structure of receptors, such as

Table 3 Literature values for human articular cartilage compression properties

Reference	Method and parameter	Articular cartilage	Modulus (MPa)
Lebourg et al. [11]	Unconfined compression, relaxation Young's modulus	–	[8.4–15.3]
Varga et al. [39]	Unconfined compression, Impact tangent modulus	–	[4–87.5] in strain range [0–0.3]
Bayraktar et al. [40]	Experimental and finite element modeling	Human femoral head	35–86

integrins, which are responsible for cell attachment, migration, and signaling [37]. Furthermore, the absence of remaining salt crystals in the SEM figures suggests that the dissolution of the salt was completed and that the pores were well interconnected. Compared to the various conventional and combinatory salt leaching techniques, the combination of a homogeneous (co-continuous) blend and salt particulate leaching will allow better interconnection between the pores made by the salt leaching and the interconnected porous structure resulting from the selective polymer leaching, since the pore walls, between the leached NaCl particles pores, are porous (due to PEO leaching) [14]. Compression molded PCL/NaCl binary blends lack pore interconnectivity as evidenced by the entrapped salt particles remaining after scaffold leaching (Fig. 7); thus clearly showing the effect of PEO on complete salt extraction and pore interconnectivity in the present molding approach. It is worthwhile mentioning here that the co-continuous polymer blend structure also speeds up the salt release process [14]. These results clearly confirm that the addition of a continuous polymer porogen overcomes one of the main disadvantages of conventional salt leaching techniques, which is the lack of interconnection between the porogen particles that leads to incomplete extraction of the porogen phase particularly at low salt concentrations.

The fabricated scaffolds showed typical stress–strain behavior of porous polymeric foams under compression consisting of four zones: toe, linear elastic, plateau, and densification [38]. Factors affecting the shape of the curves obtained from the scaffolds include the amount of porosity, pore size and morphology, and type and composition of scaffold material [38]. The three different investigated structures display different curves due to differences in pore morphology, porosity, and pore size. The co-continuous scaffolds with cylindrical walls represent the stiffest and strongest scaffolds due to thicker pore walls; whereas the scaffolds produced using the additional salt particles show the lowest modulus and strength due to thinner walls and higher porosity. In addition to that, densification begins at larger strains in the scaffolds with higher porosity. The co-continuous scaffolds molded at 100°C have much higher modulus and strength than the scaffolds molded at the lower temperature, despite the fact that they did not have significant difference in porosity. Results from this research are in agreement with results from previous studies [18] where higher compressive modulus and strength were reported with increase in pore diameter at equal porosities for co-continuous PLLA scaffolds annealed for 1 h.

The fabricated PCL scaffolds had compressive modulus values in the same range as those reported in the literature for human hyaline cartilage (Table 3). Such results confirm that the scaffolds fabricated through the integration of cryomilling, compression molding, and porogen leaching are viable candidates for load bearing applications, such as cartilage tissue engineering, at least on the mechanical rigidity point of view. This is an important factor in tissue engineering to avoid stress shielding (cells not being subjected to any stress) in the case of implants with significantly high modulus on one hand, and to avoid implanted cells and new tissue being squeezed in the case of implants with very low modulus, on the other hand. Moreover, the biomechanical environment has a strong influence on cell metabolism and phenotypic expression; thus, affecting the regeneration potential of the synthetic tissue [11]. Furthermore, the slow in vivo degradation of PCL [33] is well-suited with cartilage tissue limited healing ability.

Finally, the DSC results demonstrated that the fabricated PCL scaffolds were highly crystalline (Xc = 63–83%), showing higher melting temperatures and crystallinities after fabrication (1st heating scan) than after cooling from melt (2nd heating scan), except for the PCL scaffold molded at 60°C. The former result may be accredited to slower cooling rates during fabrication and, thus, to the presence of larger, more perfect crystals [41]. Furthermore, the melting peaks in the 1st scans consist of multiple peaks (Fig. 9a) which is attributed to multimodal crystal size distribution [42], with small size, less perfect crystals melting at lower temperatures and/or crystal reorganization (crystal perfection) during melting [41]. On the other hand, the melting peaks in the 2nd heating scans only show a low-temperature tail (Fig. 9b), which is ascribed to dispersion of crystal sizes [42]. Similar trends have been reported for PCL porous membranes fabricated by a freeze-extraction method [42]. The differences between results of the PCL from scaffolds fabricated at the same temperature (60°C) but one with salt addition and less PCL content are harder to explain. One possible explanation is that large PCL crystals formed on salt interfaces during fabrication [43], increasing the crystallinity of PCL and its melting

temperature. Other experiments are necessary to provide more insight into the origin of these differences.

5 Conclusions

This study reports on the production and characterization of scaffolds made from PCL produced via cryomill compounding, compression molding, and porogen leaching. The motivation of this research was to develop and produce a new range of scaffolds with appropriate structure and properties for load bearing applications using a scalable, economical, and solventless production approach. PCL with PEO and NaCl porogens was chosen as a model system for this study. Most of the approaches reported by previous studies to produce scaffolds from blends or composites involve the use of solvents or high temperature mixing; this work is the first reporting on the approach of using solid-state blending. The methodology described in the study is very versatile, avoids the drawbacks associated with solvent use, allows the production of a variety of scaffolds using different polymers, and permits large scale production of porous scaffolds of many sizes in an economical way.

Scaffolds were made from PCL in a fully interconnected porous structure aiming at load bearing tissue engineering applications. PCL porous scaffolds with porosity levels of $\sim 50\%$ which have been increased by mixing salt with the blend ($\sim 70\%$ for 60% wt% NaCl), and a compressive modulus and strength ($\varepsilon = 10\%$) of 60 and 2.8 MPa respectively have been fabricated. Results confirmed that the fabricated scaffolds are viable candidates for load bearing applications, such as cartilage tissue engineering. Combining polymer and salt particulate leaching in co-continuous blends allowed better interconnection between the pores, thus yielding full pore network interconnectivity in addition to higher porosities while maintaining good mechanical integrity. From these studies, future modifications can be determined to optimize the properties of scaffolds for cartilage tissue engineering.

Acknowledgments The authors acknowledge the Texas Tech University Imaging Center, Department of Biological Sciences at Texas Tech University for use of the Hitachi S-4300SE/N (NSF MRI 04-511).

References

1. Lee MH, Arcidiacono JA, Bilek AM, Wille JJ, Hamill CA, Wonnacott KM, et al. Considerations for tissue-engineered and regenerative medicine product development prior to clinical trials in the United States. Tissue Eng Part B Rev. 2009;1–14.
2. Williams DJ, Sebastine IM. Tissue engineering and regenerative medicine: manufacturing challenges. IEE Proc Nanobiotechnol. 2005;152:207–10.
3. Gabay O, Sanchez C, Taboas JM. Update in cartilage bio-engineering. Joint Bone Spine. 2010;77(4):283–6.
4. Stoddart MJ, Grad S, Eglin D, Alini M. Cells and biomaterials in cartilage tissue engineering. Regen Med. 2009;4(1):81–98.
5. Tanaka Y, Yamaoka H, Nishizawa S, Nagata S, Ogasawara T, Asawa Y, et al. The optimization of porous polymeric scaffolds for chondrocyte/atelocollagen based tissue-engineered cartilage. Biomaterials. 2010;31:4506–16.
6. Ikeda R, Fujioka H, Nagura I, Kokubu T, Toyokawa N, Inui A, et al. The effect of porosity and mechanical property of a synthetic polymer scaffold on repair of osteochondral defects. Int Orthop. 2009;33:821–8.
7. Leung L, Perron J, Naguib HE. A study of the mechanics of porous PLGA 85-15 scaffold in compression. Polym Polym Compos. 2007;15(6):437–43.
8. Jell G, Verdejo R, Safinia L, Shaffer MS, Stevens MM, Bismarck A. Carbon nanotube-enhanced polyurethane scaffolds fabricated by thermally induced phase separation. J Mater Chem. 2008;18:1865–72.
9. Shin HJ, Lee CH, Cho IH, Kim Y-J, Lee Y-J, Kim IA, et al. Electrospun PLGA nanofiber scaffolds for articular cartilage reconstruction: mechanical stability, degradation and cellular responses under mechanical stimulation in vitro. J Biomater Sci Polymer Edn. 2006;17(1–2):103–19.
10. Martinez-Diaz S, Garcia-Giralt N, Lebourg M, Gómez-Tejedor J-A, Vila G, Caceres E, et al. In vivo evaluation of 3-dimensional polycaprolactone scaffolds for cartilage repair in rabbits. Am J Sports Med. 2010;38:509–19.
11. Lebourg M, Sabater Serra R, Más Estellés J, Hernández Sánchez F, Gómez Ribelles JL, Suay Antón J. Biodegradable polycaprolactone scaffold with controlled porosity obtained by modified particle-leaching technique. J Mater Sci Mater Med. 2008;19:2047–53.
12. Woodfield TB, Malda J, De Wijn J, Peters F, Riesle J, Van Blitterswijk CA. Design of porous scaffolds for cartilage tissue engineering using a three-dimensional fiber-deposition technique. Biomaterials. 2004;25:4149–61.
13. Woodfield TB, Guggenheim M, Von Rechenberg B, Riesle J, Van Blitterswijk CA, Wedler V. Rapid prototyping of anatomically shaped, tissue-engineered implants for restoring congruent articulating surfaces in small joints. Cell Prolif. 2009;42(4):485–97.
14. Reignier J, Huneault MA. Preparation of interconnected poly(ε-caprolactone) porous scaffolds by a combination of polymer and salt particulate leaching. Polymer. 2006;47:4703–17.
15. Washburn NR, Simon CG, Tona A, Elgendy HM, Karim A, Amis EJ. Co-extrusion of biocompatible polymers for scaffolds with co-continuous morphology. J Biomed Mater Res. 2002;60(1):20–9.
16. Sarazin P, Favis BD. Morphology control in co-continuous poly(L-lactide)/polystyrene blends: a route towards highly structured and interconnected porosity in poly(L-lactide) materials. Biomacromolecules. 2003;4:1669–79.
17. Yuan Z, Favis BD. Macroporous poly(l-lactide) of controlled pore size derived from the annealing of co-continuous polystyrene/poly(l-lactide) blends. Biomaterials. 2004;25:2161–70.
18. Sarazin P, Roy X, Favis BD. Controlled preparation and properties of porous poly(L-lactide) obtained from a co-continuous blend of two biodegradable polymers. Biomaterials. 2004;25:5965–78.
19. Sarazin P, Virgilio N, Favis BD. Influence of the porous morphology on the in vitro degradation and mechanical properties of poly(L-lactide) disks. J Appl Polym Sci. 2006;100(2):1039–47.
20. Zhu YG, Li ZQ, Zhang D, Tanimoto T. Abs-iron nanocomposites prepared by cryomilling. J Appl Polym Sci. 2006;99:501–5.
21. Zhu YG, Li ZQ, Gu JJ, Zhang D, Tanimoto T. Polyaniline-iron nanocomposites prepared by cryomilling. J Polym Sci B Polym Phys. 2006;44:3157–64.
22. Smith AP, Ade H, Koch CC, Spontak RJ. Solid-state blending of polymers by cryogenic mechanical alloying. In: Anastasiadis SH,

Karim A, Ferguson GS, editors. Materials research society symposium 2000;629. p. FF691-6.
23. Vertuccio L, Gorrasi G, Sorrentino A, Vittoria V. Nano clay reinforced PCL/starch blends obtained by high energy ball milling. Carbohydr Polym. 2009;75:172–9.
24. Chen Z, Wang Q. Pan-milling mixing—a novel approach to forming polymer blends and controlling their morphology. Polym Int. 2001;50(9):966–72.
25. Masuda J, Torkelson JM. Dispersion and major property enhancements in polymer/multiwall carbon nanotube nanocomposites via solid-state shear pulverization followed by melt mixing. Macromolecules. 2008;41:5974–7.
26. Tao Y, Kim J, Torkelson JM. Achievement of quasi-nanostructured polymer blends by solid-state shear pulverization and compatibilization by gradient copolymer addition. Polymer. 2006;47:6773–81.
27. Suryanarayana C. Mechanical alloying and milling. Prog Mater Sci. 2001;46:1–184.
28. Zhu YG, Li ZQ, Zhang D, Tanimoto T. PET-SiO_2 nanocomposites prepared by cryomilling. J Polym Sci B Polym Phys. 2006;44:1161–7.
29. Martin, JP. An investigation of the microstructure and properties of a cryogenically mechanically alloyed polycarbonate-poly(ether ether ketone) system [Dissertation]. Blacksburg (VA): Virginia Polytechnic Institute and State University; 2001. Available from URL: http://scholarlibvtedu/theses/available/etd-11292001-141959/.
30. Smith AP, Spontak RJ, Ade H, Smith SD, Koch CC. High-energy cryogenic blending and compatibilizing of immiscible polymers. Adv Mater. 1999;11(15):1277–81.
31. Wan Y, Wu H, Cao X, Siqin Dalai S. Compressive mechanical properties and biodegradability of porous poly(caprolactone)/chitosan scaffolds. Polym Degrad Stabil. 2008;93:1736–41.
32. Eastmond GC. Poly(ε-caprolactone) Blends. In: Advances in Polymer Science: Biomedical Applications/Polymer Blends; 149. New York: Springer Berlin-Heidelberg; 2000, p. 59–223.
33. Mano JF, Sousa RA, Boesel LF, Neves NM, Reis RL. Bioinert, biodegradable and injectable polymeric matrix composites for hard tissue replacement: state of the art and recent developments. Compos Sci Technol. 2004;64:789–817.
34. Terife G, Narh KA. Creating polymer-carbon nanotubes nanocomposites by cryomilling. ANTEC 2009 Plastics: Annual Technical Conference Proc. 2009;1:349–53.
35. Sorrentino A, Gorrasi G, Tortora M, Vittoria V, Costantino U, Marmottini F, et al. Incorporation of Mg–Al hydrotalcite into a biodegradable Poly(ε-caprolactone) by high energy ball milling. Polymer. 2005;46:1601–8.
36. Gross KA, Rodriguez-Lorenzo LM. Biodegradable composite scaffolds with an interconnected spherical network for bone tissue engineering. Biomaterials. 2004;25:4955–62.
37. Beskardes IG, Gümüsderelioglu M. Biomimetic apatite-coated PCL scaffolds: effect of surface nanotopography on cellular functions. J Bioact Compat Polym. 2009;24:507–24.
38. Correlo VM, Boesel LF, Pinho E, Costa-Pinto AR, Alves da Silva ML, Bhattacharya M, et al. Melt-based compression-molded scaffolds from chitosan/polyester blends and composites: morphology and mechanical properties. J Biomed Mater Res A. 2009;91(2):489–504.
39. Varga F, Drzík M, Handl M, Chlpík J, Kos P, Filová E, et al. Biomechanical characterization of cartilages by a novel approach of blunt impact testing. Physiol Res. 2007;56(Suppl 1):S61–8.
40. Bayraktar HH, Morgan EF, Niebur GL, Morris GE, Wong EK, Keaveny TM. Comparison of the elastic and yield properties of human femoral trabecular and cortical bone tissue. J Biomech. 2004;37:27–35.
41. Menczel JD, Judovits L, Prime RB, Bair HE, Reading M, Swier S. Differential scanning calorimetry (DSC). In: Menczel JD, Prime RB, editors. Thermal analysis of polymers: fundamentals and applications. New Jersey: Wiley; 2009. p. 7–239.
42. Lebourg M, Anton JS, Gomez Ribelles JL. Porous membranes of PLLA–PCL blend for tissue engineering applications. Eur Polym J. 2008;44:2207–18.
43. Tracz A, Kucinska I, Jeszka JK. Unusual crystallization of polyethylene at melt/atomically flat interface: lamellar thickening growth under normal pressure. Polymer. 2006;47:7251–8.